Prepared for submission to JCAP

Forecasts for CMB μ and i-type spectral distortion constraints on the primordial power spectrum on scales $8 \lesssim k \lesssim 10^4$ Mpc^{-1} with the future Pixie-like experiments

Rishi Khatri,[a] **Rashid A. Sunyaev**[a,b]

[a]Max Planck Institut für Astrophysik
, Karl-Schwarzschild-Str. 1 85741, Garching, Germany
[b]Space Research Institute, Russian Academy of Sciences, Profsoyuznaya 84/32, 117997 Moscow, Russia

E-mail: khatri@mpa-garching.mpg.de

Abstract. Silk damping at redshifts $1.5 \times 10^4 \lesssim z \lesssim 2 \times 10^6$ erases CMB anisotropies on scales corresponding to the comoving wavenumbers $8 \lesssim k \lesssim 10^4$ Mpc^{-1}. This dissipated energy is gained by the CMB monopole, creating distortions from a blackbody in the CMB spectrum of the μ-type and the i-type. We study, using Fisher matrices, the constraints we can get from measurements of these spectral distortions on the primordial power spectrum from future experiments such as Pixie, and how these constraints change as we change the frequency resolution and the sensitivity of the experiment. We show that the additional information in the shape of the i-type distortions, in combination with the μ-type distortions, allows us to break the degeneracy between the amplitude and the spectral index of the power spectrum on these scales and leads to much tighter constraints. We quantify the information contained in both the μ-type distortions and the i-type distortions taking into account the partial degeneracy with the y-type distortions and the temperature of the blackbody part of the CMB. We also calculate the constraints possible on the primordial power spectrum when the spectral distortion information is combined with the CMB anisotropies measured by the WMAP, SPT, ACT and Planck experiments.

Keywords: cosmic background radiation, cosmology:theory, early universe

Contents

1 The spectrum of CMB

In the early Universe, at redshifts $z \gg 2 \times 10^6$, there is almost perfect thermal equilibrium between photons and electrons/baryons which maintains the spectrum of the cosmic microwave background (CMB) to be a blackbody spectrum even in the presence of enormous energy injection such as during electron-positron annihilation. This prediction of the standard big bang cosmological model was confirmed by the Far Infrared Absolute Spectrophotometer (FIRAS) instrument on the Cosmic Background Explorer satellite (COBE) [1] which found that the CMB is indeed blackbody to high precision. If there is any energy injection into (or cooling of) the primordial plasma at $z \gtrsim 2 \times 10^6$, Compton scattering is able to very quickly redistribute this excess (or deficit) of energy over the entire spectrum of photons restoring the equilibrium Bose-Einstein distribution [2] with chemical potential parameter μ and occupation number $n(x) = 1/(e^{x+\mu} - 1)$, where $x = h\nu/k_{\rm B}T$, h is Planck's constant, $k_{\rm B}$ is Boltzmann's constant, ν is the photon frequency and T is the temperature of photons and baryons. The chemical potential is in turn driven to zero by photon production [2] by bremsstrahlung and, more importantly for a low baryon density Universe such as ours, by double Compton scattering [3]. Electrons are also maintained at the equilibrium Maxwellian distribution by Compton scattering with the photons [4, 5] whose number density exceeds that of the electrons by a factor of $\sim 10^9$. Coulomb collisions efficiently maintain equilibrium between electrons and ions in the entire redshift range of interest to us and they can be assumed to have the same temperature, defined by the photon spectrum[4, 5], Eq. A.1.

At redshifts $z \lesssim 2 \times 10^6$, bremsstrahlung and double Compton scattering become inefficient in creating photons, however Compton scattering is still able to maintain kinetic equilibrium (Bose-Einstein spectrum) until $z \approx 2 \times 10^5$. This, therefore, defines the era where it is possible to create μ-type distortions with the μ parameter related to the fractional energy Q ($\equiv \Delta E/E_\gamma$, where ΔE is the energy density going into the spectral distortions and $E_\gamma = a_{\rm R}T^4$ is the energy density of radiation and $a_{\rm R}$ is the radiation constant) injected into the radiation by[2, 6] $\mu = 1.4Q$. To calculate the μ-type distortions it is necessary to calculate precisely the suppression of μ behind the blackbody surface at $z \approx 2 \times 10^6$. This is of course possible with the numerical codes such as CosmoTherm[1] [7] and KYPRIX[8], the former code includes precise calculation of distortions arising from the energy injection due to Silk damping. Sunyaev and Zeldovich [2] found an analytic solution for the suppression factor or blackbody visibility $e^{-\mathcal{T}(z)}$ and this solution was recently made even more precise [9], allowing a fast and accurate computation of μ-type distortions. These analytic solutions

[1] www.chluba.de/CosmoTherm

and the recipe for using them are given in Appendix A. COBE 95% confidence level limit on the μ parameter is $\mu < 9 \times 10^{-5}$ [1].

At redshifts $z \lesssim 2 \times 10^5$, Compton scattering is not sufficient to maintain a Bose-Einstein spectrum in the presence of energy injection and is able to move the spectrum only partially towards the equilibrium creating intermediate or *i*-type distortions at redshifts $z \gtrsim 1.5 \times 10^4$. The distortions in this epoch must be calculated numerically by solving the Kompaneets equation [10]. This was done in Ref. [11] and the results are publicly available. The recipe for using these results to calculate the *i*-type part of spectral distortions for a general energy injection scenario is given in Appendix A. We refer to [11] for a detailed discussion of the *i*-type distortions and how they can help distinguish between different energy injection scenarios, for example energy injection rate which is exponential in redshift such as particle decay, and that which is a power law such as Silk damping. We should emphasize that an *i*-type component is inevitable for power law energy injection such as Silk damping (which itself is unavoidable) while a particle decay can happen entirely in the μ epoch leading to negligible *i*-type distortions. Thus the presence of absence of *i*-type distortions together with the shape of the *i*-type distortions is a powerful discriminant for different energy injection mechanisms.

At redshifts $z \lesssim 1.5 \times 10^4$, comptonization is minimal, and the solution for the distortions is given by a *y*-type distortion [12], which are also created at lower redshifts when the CMB photons are scattered in the clusters of galaxies by hot electrons. The *y*-type distortions are expected to be dominated by low redshift contributions coming from the epoch of reionization, with y parameter (see Eqs. 3.1,A.8) given by $y \sim 10^{-7}$, and warm hot intergalactic medium [11, 13–20] with $y \sim 10^{-6} - 10^{-7}$. The *y*-type distortions are therefore hard to predict and must be fitted as a free parameter during the Fisher matrix analysis. COBE 95% limit on the *y* parameter is $y < 1.5 \times 10^{-5}$ [1]. However, a future experiment such as Cosmic Origins Explorer (COrE) [21] may be able to detect compact sources of *y*-type distortion and thus help estimate and clean the low redshift average *y*-type distortion contribution.

There are spectral distortions, other than *y*, μ and *i*-type, which are created in the CMB, for example, recombination lines from the epoch of recombination [22–26] and in CMB anisotropies from resonant scattering of the CMB in metals lines during reionization and later [27], which we will not discuss here. We refer to a recent review [28] for a more complete discussion of the various spectral distortions in the CMB.

2 Spectral distortions from Silk damping: Observing 17 e-folds of inflation

Photons diffusing through the primordial plasma erase perturbations on small scales [31–33] and this effect, known as Silk damping, has already been observed in the CMB anisotropies by the Atacama Cosmology Telescope[34] (ACT), the South Pole Telescope[35] (SPT), and now the Planck experiment [36] on scales up to $k \approx 0.2\text{Mpc}^{-1}$, which is also the damping scale at $z \approx 1200$, where the anisotropies are suppressed but not completely erased. The wavenumbers corresponding to the photon diffusion length are $k_{\rm D} \approx 10^4\text{Mpc}^{-1}$ (or multipole $\ell \approx 10^8$) at $z = 2 \times 10^6$ and $k_{\rm D} \approx 8\text{Mpc}^{-1}$ ($\ell \approx 10^5$) at $z = 1.5 \times 10^4$, and on these very small scales the anisotropies are almost completely erased from the CMB and are therefore unobservable in the CMB anisotropy power spectrum. The energy stored in the perturbations (or the sound waves in the primordial radiation pressure dominated plasma) on the dissipating scales, however, does not disappear but goes into the monopole spectrum creating *y*, μ and *i*-type distortions, see Fig. 1. This effect was estimated initially by Sunyaev and Zeldovich [2] and later by Daly [37] and Hu, Scott and Silk [38]. Recently, the energy dissipated in Silk damping and going into the spectral distortions was calculated precisely in [39], correcting previous calculations and also giving a clear physical interpretation of the effect in terms of mixing of

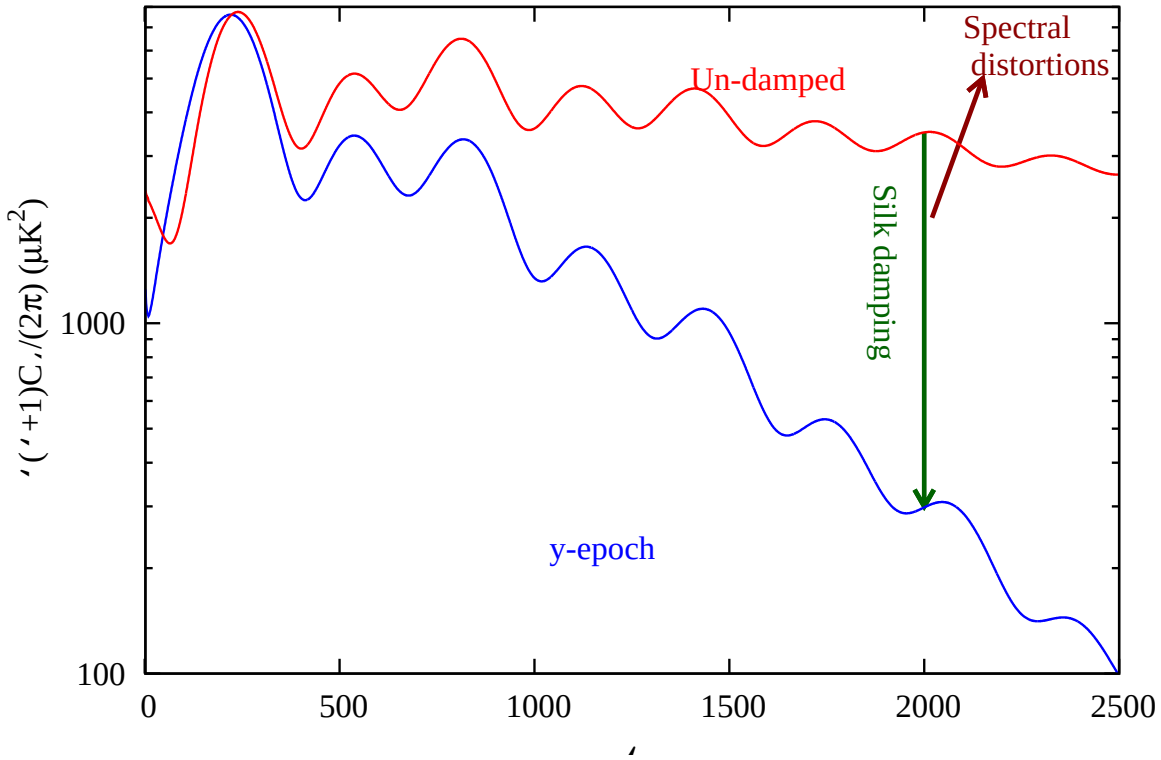

Figure 1. Power which disappears from the anisotropies appears in the monopole as spectral distortions. CMB power spectrum calculated using CMBFAST [29] with the undamped spectrum estimated by enforcing tight coupling in the code during recombination and cutting off the line of sight integral at $z = 800$. See also [30].

blackbodies [39, 40] [2]. The calculations in [39] showed that photon diffusion just mixes blackbodies and the resulting distortion is a y-type distortion which can comptonize into i-type or μ-type distortion, depending on the redshift. We can write down the (fractional) dissipated energy ($Q \equiv \Delta E/E_\gamma$) going into the spectral distortions as [39, 40]

$$\frac{\mathrm{d}Q}{\mathrm{d}t} = -2\frac{\mathrm{d}}{\mathrm{d}t}\int \frac{k^2\mathrm{d}k}{2\pi^2} P_i^\gamma(k)\left[\sum_{\ell=0}^{\infty}(2\ell+1)\Theta_\ell^2\right] \approx -2\frac{\mathrm{d}}{\mathrm{d}t}\int \frac{k^2\mathrm{d}k}{2\pi^2} P_i^\gamma(k)\left[\Theta_0^2 + 3\Theta_1^2\right], \qquad (2.1)$$

where $\Theta_\ell(k)$ are the spherical harmonic multipole moments of temperature anisotropies of the CMB, t is proper time and $P_i^\gamma(k) = \frac{4}{0.4R_\nu+1.5}P_\zeta \approx 1.45P_\zeta$, $P_\zeta = (A_\zeta 2\pi^2/k^3)(k/k_0)^{n_\mathrm{s}-1+\frac{1}{2}\mathrm{d}n_\mathrm{s}/\mathrm{d}\ln k(\ln k/k_0)}$, the amplitude of comoving curvature perturbation A_ζ is equivalent to Δ_R^2 in Wilkinson Microwave Anisotropy Probe (WMAP) papers [43], and $R_\nu = \rho_\nu/(\rho_\nu+\rho_\gamma) \approx 0.4$, ρ_ν is the initial neutrino energy density and ρ_γ is the initial photon energy density, but after electron positron annihilation [44], k_0 is the pivot point, n_s is the spectral index and $\mathrm{d}n_\mathrm{s}/\mathrm{d}\ln k$ is its running [45, 46]. The last approximate equality is valid in the tight coupling approximation when the energy in the multipole moments $\ell \geq 2$ can be neglected.

It is possible to evaluate the time derivative in Eq. 2.1 explicitly using the first order Boltzmann equation for photons, yielding an exact expression in terms of photon quadrupole, dipole and higher order multipoles and baryon peculiar velocity which is valid at all times [39, 40]. But in the redshift

[2] See [41] for a slightly different way of calculating μ-type distortions and also [42].

range of interest to us, $z \gtrsim 1.5 \times 10^4$, the tight coupling solutions are quite accurate [47, 48], yielding the following expression for the energy injection rate [39, 49],

$$\frac{\mathrm{d}Q}{\mathrm{d}z} = \frac{9}{4}\frac{\mathrm{d}(1/{k_\mathrm{D}}^2)}{\mathrm{d}z}\int \frac{\mathrm{d}^3k}{(2\pi)^3} P^i_\gamma(k) k^2 e^{-2k^2/{k_\mathrm{D}}^2}, \tag{2.2}$$

where k_D is the damping wavenumber given by [31–33, 50],

$$\frac{1}{{k_\mathrm{D}}^2} = \int_z^\infty \mathrm{d}z \frac{c(1+z)}{6H(1+R)n_\mathrm{e}\sigma_\mathrm{T}}\left(\frac{R^2}{1+R} + \frac{16}{15}\right), \tag{2.3}$$

where $R \equiv \frac{3\rho_b}{4\rho_\gamma}$, ρ_b is the baryon energy density, σ_T is Thomson cross section, m_e is the mass of electron, n_e is the number density of electrons, c is the speed of light, and H is the Hubble parameter. In general the Eqs. 2.2 and 2.3 must be evaluated numerically. However in the radiation dominated epoch, $R \ll 1$ and for a power law initial power spectrum, $\mathrm{d}n_\mathrm{s}/\mathrm{d}\ln k = 0$, we can evaluate the integrals analytically yielding,

$$\frac{\mathrm{d}Q}{\mathrm{d}z} = \frac{3.25 A_\zeta}{k_0^{n_\mathrm{s}-1}}\frac{\mathrm{d}(1/{k_\mathrm{D}}^2)}{\mathrm{d}z} 2^{-(3+n_\mathrm{s})/2} {k_\mathrm{D}}^{n_\mathrm{s}+1}\Gamma\left(\frac{n+1}{2}\right). \tag{2.4}$$

Once we know the energy injection rate, it is easy to calculate the μ-type and i-type distortions using the method given in Appendix A. We should also mention that the spectral distortions from Silk damping may also permit us to constrain the primordial local type non-gaussianity on these very small scales [51, 52].

3 Fisher forecast results for Pixie-like experiments

We will now calculate the constraints we can put on the initial power spectrum using CMB spectral distortions. Although the spectral distortions are sensitive to cosmological parameters other than the power spectrum, as can be seen from the equations, these sensitivities are relatively milder and we know the other cosmological parameters to high accuracy from CMB anisotropy and other data [34, 35, 43, 53–62]. We will therefore fix all parameters, except for the power spectrum, to the following values for flat ΛCDM cosmology[43]: CMB temperature $T_\mathrm{CMB} = 2.725$ K, baryon density parameter $\Omega_\mathrm{b} = 0.0458$, cold dark matter $\Omega_\mathrm{cdm} = 0.229$, Hubble constant $h_0 = 0.702$, helium fraction 0.24, effective number of neutrinos[63] 3.046.

We can write down the spectral distortion of CMB, ΔI_ν, which will be measured by Pixie [64] as

$$\Delta I_\nu = tI^t_\nu + yI^y_\nu + I^\mathrm{damping}_\nu(n_\mathrm{s}, A_\zeta, \mathrm{d}n_\mathrm{s}/\mathrm{d}\ln k). \tag{3.1}$$

The first term is the uncertainty in the temperature of the blackbody part of the spectrum which is not known a priori and must be fit simultaneously with the spectral distortions, second term is the y-type distortion which has contributions from low redshift intergalactic medium and is therefore a free parameter. The last term is the i-type + μ-type distortions from the dissipation of acoustic modes and is a function of the power spectrum which we parmeterize by the amplitude, the spectral index and its running. The formulae for different terms in Eq. 3.1 are given in Appendix A. If there is new physics injecting energy, there will be additional terms added to the above distortion. For example, if there is decay of particles before $z = 2 \times 10^5$, it will create additional μ-type distortions and a term μI^μ_ν should be fitted with μ as a free parameter. Adding additional parameters will of course

degrade the constraints on the primordial power spectrum and we will discuss it briefly below. We should also include cooling of CMB due to energy transfer to baryons which cool faster than radiation [7, 22, 23, 49], however, it depends only on cosmological parameters which we have assumed to be constant and therefore does not affect the Fisher matrix. The cooling must be included in a precise calculation using, for example, Markov chain Monte Carlo to explore the likelihood.

If $\Delta\nu$ is the spectral resolution of the experiment and $\delta I(\nu)$ is the noise in each channel, the Fisher matrix is given by (e.g. [65–67]),

$$F_{\alpha\beta} = \sum_j \frac{1}{\delta I(\nu_j)^2} \frac{\partial \Delta I_\nu}{\partial \theta_\alpha}(\nu_j) \frac{\partial \Delta I_\nu}{\partial \theta_\beta}(\nu_j), \tag{3.2}$$

where ν_j is the center frequency of each channel, $\theta_{\alpha,\beta} \in (t, y, n_s, A_\zeta, \mathrm{d}n_s/\mathrm{d}\ln k)$, and the sum is over all frequency channels which we take to be from 30 GHz to 500 GHz. The upper limit of the usable frequency range will depend on how well we can remove the foregrounds which become more problematic at higher frequencies. In the analysis below we will assume that the foregrounds have been removed at required precision ($\sim \delta I$) using the frequency channels greater than 500 GHz which is the plan for the Pixie experiment [64]. In the Pixie proposal $\Delta\nu = 15$ GHz, with a total of 400 frequency channels extending to 6 THz and the hope is that the large number of channels at high frequencies would help nail down the foregrounds to the desired accuracy.

It is extremely important to study the impact the foregrounds have on the ability of Pixie-like experiments to detect spectral distortion but which is beyond the scope of present work. This paper is only a first step in quantifying the information content and the detectability of the spectral distortions with respect to constraining the primordial power spectrum on scales $8\ \mathrm{Mpc}^{-1} \lesssim k \lesssim 10^4\ \mathrm{Mpc}^{-1}$.

The covariance matrix is just the inverse of the Fisher matrix, $cov_{\alpha\beta} = \left[F^{-1}\right]_{\alpha\beta}$ If we are interested in only first n parameters of the parameter vector θ, we can marginalize over the rest of the parameters by writing the Fisher matrix as

$$\begin{pmatrix} A & B \\ B^T & C \end{pmatrix}, \tag{3.3}$$

where the sub-matrix A spans over the parameters we are interested in. The marginalized Fisher matrix is then given by $\bar{F} = A - BC^{-1}B^T$. It can also be obtained (if the parameters are non-degenerate) by taking the rows and columns of the parameters we are interested in from the covariance matrix and inverting the resulting sub-matrix. If we want to fix some parameter at a particular value instead of marginalizing over it, we just eliminate the row and column for that parameter from the Fisher matrix. The marginalized $\nu - \sigma$ ellipsoids are then given by $\Delta\theta^T \bar{F} \Delta\theta = \chi^2(\nu)$ where $\Delta\theta = \theta - \theta_{\mathrm{fiducial}}$ and the Fisher matrix is also evaluated at the fiducial values of the parameters. For two parameters, $\chi^2(1) = 2.3, \chi^2(2) = 6.17$.

Let us first consider the constraints we can obtain from spectral distortions alone. For this we take the pivot point $k_0 = 42\ \mathrm{Mpc}^{-1}$, which is approximately in the middle of the i-type distortions epoch, and constrain the amplitude and the spectral index on small scales (without running and large scale power spectrum constraints). We thus have the parameter vector $\theta = (n_s(k_0 = 42\ \mathrm{Mpc}^{-1}), A_\zeta(k_0 = 42\ \mathrm{Mpc}^{-1}), t, y)$. We take the fiducial model $n_s(k_0 = 42\ \mathrm{Mpc}^{-1}) = 0.96, A_\zeta(k_0 = 42\ \mathrm{Mpc}^{-1}) = 1.61 \times 10^{-9}$ and marginalize over t and y. The resulting 68% contours are shown in Fig. 2 for Pixie [64] spectral resolution $\delta\nu = 15$GHz and sensitivity $\delta I(\nu) = 5 \times 10^{-26} \mathrm{Wm}^{-2}\mathrm{Sr}^{-1}\mathrm{Hz}^{-1}$. We also show the contours obtained by increasing the spectral resolution to 1 GHz or/and sensitivity to $\delta I(\nu) = 10^{-26} \mathrm{Wm}^{-2}\mathrm{Sr}^{-1}\mathrm{Hz}^{-1}$. We should emphasize that these are completely independent constraints on the power spectrum on scales $8\ \mathrm{Mpc}^{-1} \lesssim k \lesssim 10^4\ \mathrm{Mpc}^{-1}$, where there are currently

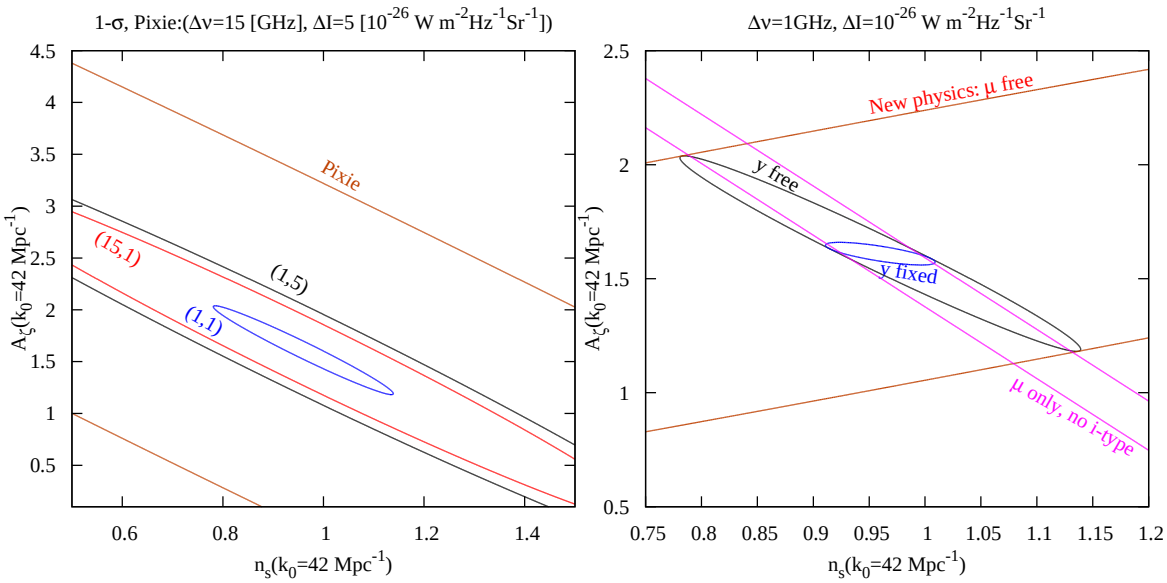

Figure 2. Marginalized Fisher matrix constraints on amplitude and spectral index of primordial power spectrum defined with respect to the pivot point $k_0 = 42$ Mpc^{-1}. Left panel shows constraints for different spectral resolutions and sensitivities of Pixie-like experiments. The labels for different contours are resolution in units of GHz and δI in units of Wm^{-2}Sr^{-1}Hz^{-1}, $(\Delta\nu, \delta I)$. Right panel demonstrates degeneracies between different parameters for resolution 1 GHz and sensitivity Wm^{-2}Sr^{-1}Hz^{-1}. The curve labeled *y* free is the normal contour we expect marginalized over *y* and *t*. If we ignore the information in the shape of the *i*-type distortions and consider only μ-type distortions, as in studies so far, we get the curve labeled 'μ only'. If we add an additional free parameter, μ, which may arise from new physics such as decay of particles, we get the 'μ-free' curve. The curve labeled '*y*-fixed' is the one we get if we assume we can predict and fix the *y*-type distortions from low redshifts.

absolutely no constraints. Thus, although they may look much weaker compared to the constraints from CMB anisotropies [43], they still represent significant improvement in our knowledge of the cosmological initial conditions.

The right panel in Fig. 2 demonstrates the degeneracies between different types of distortions. The curve marked '*y* free' is the same as the (1,1) curve in the left panel, marginalized over *y* and *t*. The curve labeled 'μ only, no *i*-type' is the one obtained if we ignore that the *i*-type distortions have a characteristic shape with information about the spectral index and divide all the energy released into *y*-type ($z \lesssim 5 \times 10^4$) and μ-type ($z \gtrsim 5 \times 10^4$) distortions, as in previous studies (c.f. Fig. 17 in [39]). Clearly it is not possible to constrain two parameters with one observable, μ, in this case and our two parameters are completely degenerate. Inclusion of the *i*-type distortions gives the '*y* free' curve and converts the straight line contours into an ellipse demonstrating the information contained in the shape of the *i*-type distortions. A different way of seeing this is by making the μ parameter free, for example, as a result of new physics such as decaying particles at $z \gtrsim 2 \times 10^5$. Note that we already have *y* and *t* free, so the constraints in the 'μ free' contours are coming solely from the shape of the *i*-type distortions. The fact that we can get any constraints at all in this last case demonstrates that the *i*-type distortions are not completely degenerate with and cannot be mimicked by a combination of *y*, μ distortions and *t* parameter. Finally the curve labeled '*y* fixed' is obtained by eliminating the row and column corresponding to *y* parameter from the Fisher matrix, thus fixing *y*. Comparing with '*y* free' curve, this tells us how the presence of stars and galaxies (responsible for reionization, WHIM which give low redshift *y*-distortions) in the Universe limits our ability to measure the primordial

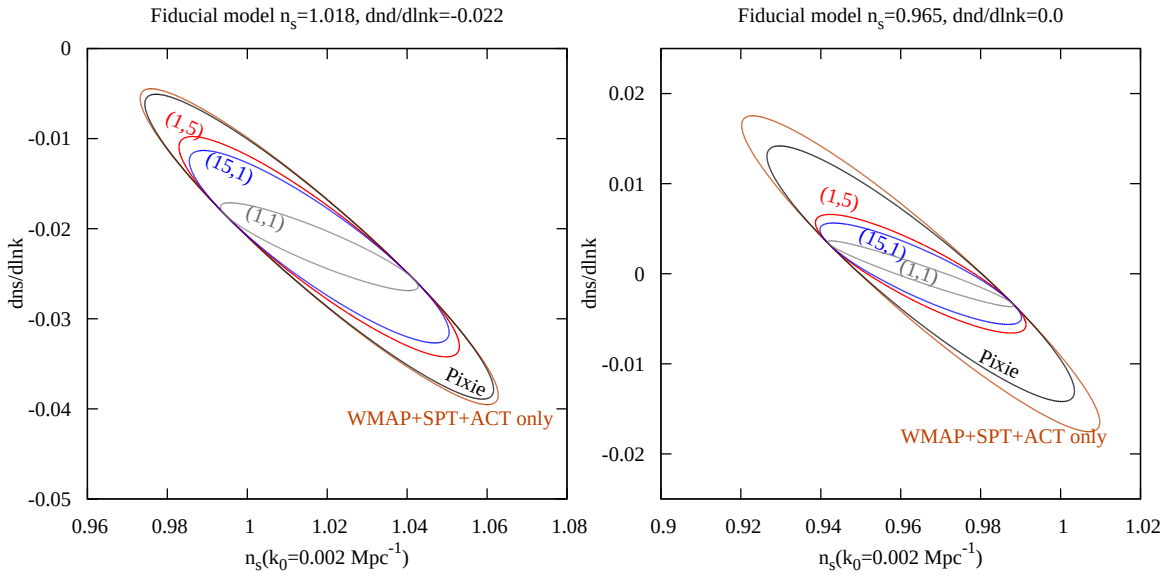

Figure 3. Constraints (68% confidence level) by combining WMAP+SPT+ACT [34, 35, 43, 53, 54] with spectral distortions from Pixie-like experiments for two different fiducial models. Labels are same as in Fig. 2. A fiducial model with zero running has more power on small scales and therefore gives tighter constraints.

power spectrum with the CMB spectral distortions.

The model considered above is perhaps the most general model we can hope to constrain with the spectral distortions. A very restrictive model on the other hand is a model with running spectral index, which applies to both the large scale anisotropies and the spectral distortion. For this model, we take the pivot point at $k = 0.002$ Mpc^{-1} as in the WMAP papers. So we can use the Markov chains provided by the WMAP team and combine the CMB anisotropy data with the spectral distortions to see how the spectral distortions improve the constraints on the spectral index and its running. We use the Markov chain with the running spectral index and including ACT [34, 54] and SPT [35, 53] data provided by the WMAP team[3] [43] and use CosmoMC [68] to extract the covariance matrix for $n_s, \mathrm{d}n_s/\mathrm{d}\ln k, A_\zeta$ from it. We use two fiducial models, one with best fit WMAP values for the running model $n_s = 1.018, \mathrm{d}n_s/\mathrm{d}\ln k = -0.022, 10^9 A_\zeta = 2.345$ and a second one with $n_s = 0.965, \mathrm{d}n_s/\mathrm{d}\ln k = 0, 10^9 A_\zeta = 2.43$ to investigate how the change in fiducial model affects the constraints. We marginalize over y, t and A_ζ and give the $1-\sigma$ contours for $n_s, \mathrm{d}n_s/\mathrm{d}\ln k$ for different spectral resolution and sensitivities for the Pixie-like experiments in Fig. 3. It is clear from this figure that spectral distortion detection would be able to improve the constraints in this simple but restrictive model. The constraints are sensitive to the fiducial model. This is expected since a fiducial model with negative running will give much smaller distortions compared to a model with zero running and the effect is amplified because of the long separation of scales between the pivot point a $k = 0.002$ Mpc^{-1} and the relevant damping scales at $k \gtrsim 8$ Mpc^{-1}.

Planck CMB experiment's cosmology results[4] are now available [36]. To estimate how an improvement in the large scale constraints on the primordial power spectrum affect the information coming from spectral distortions, we use the covariance matrix for baseline ΛCDM + running model provided by the Planck team[36] which in addition uses polarization data from WMAP [69] and high

[3] http://lambda.gsfc.nasa.gov/product/map/current/

[4] Based on observations obtained with Planck (http://www.esa.int/Planck), an ESA science mission with instruments and contributions directly funded by ESA Member States, NASA, and Canada.

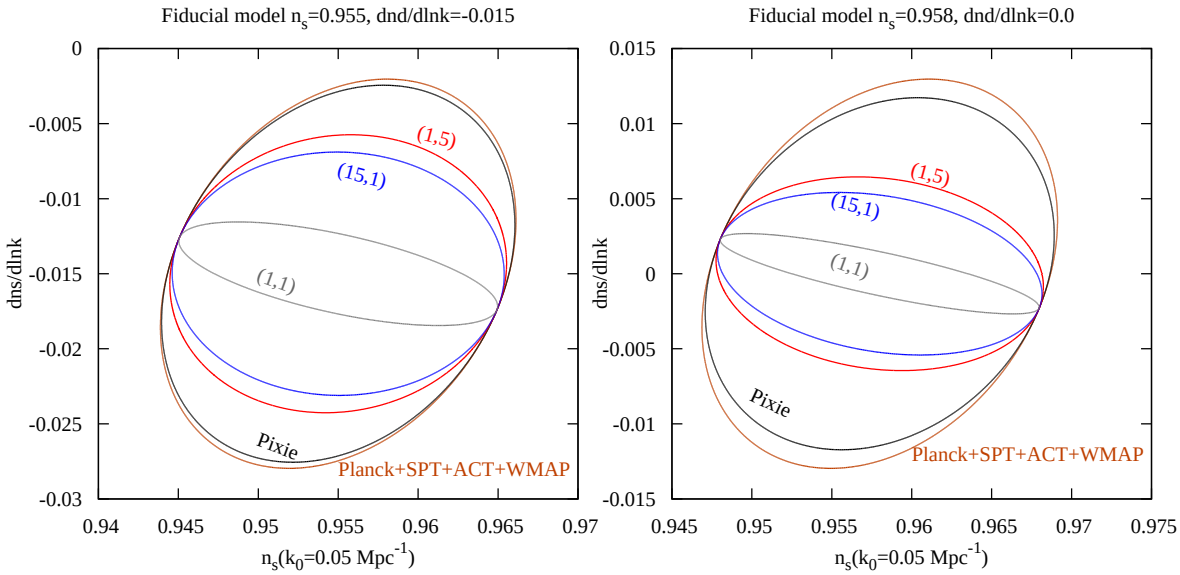

Figure 4. Constraints (68% confidence level) obtained by combining the Planck+SPT+ACT+WMAP polarization [36, 43, 70, 71] with spectral distortions from Pixie-like experiments. Labels are same as in Fig. 2. Planck mean fit parameters are used for the fiducial model in the left panel of the plot. The right panel uses a fiducial model with zero running leading to stronger spectral distortions and tighter constraints.

ℓ data from SPT [70] and ACT [71]. For combining Planck results with spectral distortions, we use the Planck mean fit parameters, $\Omega_{\rm b}h^2 = 0.02225, \Omega_{\rm cdm}h^2 = 0.1205, h = 0.672$ and fiducial model with $n_{\rm s} = 0.955, {\rm d}n_{\rm s}/{\rm d}\ln k = -0.015, \ln(10^{10}A_\zeta) = 3.12, k_0 = 0.05$ Mpc^{-1}. The results are plotted in Fig. 4. We again demonstrate the effect of fiducial model in the right panel of Fig 4 where the fiducial model is taken to be $n_{\rm s} = 0.958, {\rm d}n_{\rm s}/{\rm d}\ln k = 0, \ln(10^{10}A_\zeta) = 3.1, k_0 = 0.05$ Mpc^{-1} but the same Planck covariance matrix and other parameters as the left panel. By comparing Figs. 3 and 4 it is clear that there is additional and complementary information coming from the spectral distortions irrespective of the improvements in the large scale constraints from the CMB anisotropies.

4 Concluding remarks

We have calculated the Fisher matrix forecasts for the possible constraints on the primordial power spectrum using CMB spectral distortions arising from Silk damping. These results, of course, come with the usual caveats associated with the Fisher matrix analysis. In particular, the spectral distortions are a non-linear function of the primordial power spectrum parameters and are most likely non-Gaussian. In addition, adiabatic cooling of baryons [7, 49] reduces the signal and determines the smallest positive distortions that can be detected. Our analysis does not take this into account, since the constant terms drop out in the derivatives used to calculate Fisher matrices. For the cosmological parameters preferred by Planck, the adiabatic cooling dominates over the Silk damping for ${\rm d}n_{\rm s}/{\rm d}\ln k < -0.08$, for the total i-type + μ-type distortion, which is ruled out at high significance and our Fisher matrix calculations are a good approximation within the allowed region. Our calculation represents the first step in quantifying the information stored in the spectral distortions, in particular the i-type distortions and paves the way for a more careful analysis using Markov chain Monte Carlo techniques in the future. Fisher matrix analysis, in particular, shows approximately how much im-

provement in constraints can be expected if the spectral resolution or the sensitivity of Pixie is made better and also shows how these constraints are sensitive to the choice of fiducial models.

We have also shown that there is important information in the shape of the spectral distortions coming from the *i*-type distortions, which has so far been ignored in constraint calculations, although this information was available from the numerical computations of the spectral distortions. In particular, the *i*-type distortions are very important in breaking the degeneracy between the amplitude and the spectral index of the primordial power spectrum on the scales $8 \lesssim k \lesssim 10^4$ Mpc^{-1}. More important than the error bars on different power spectrum parameters is the fact that with spectral distortions we will be able to extend our knowledge of initial conditions to completely new scales separated by many orders of magnitude from the information available from CMB anisotropy and large scale structure data. In inflationary terms, this amounts to extending our view of inflation from ~ 6 e-folds at present to ~ 17 e-folds, which might well be a significant fraction of the full inflationary epoch.

A Recipe for the calculation of CMB spectral distortions for a general energy injection scenario

To calculate the spectral distortions arising from a given energy injection rate, dQ/dz, where $Q = \Delta E/E_\gamma$ is the fractional energy injected into the CMB, we must solve Kompaneets equation[10] including photon production and absorption due to bremsstrahlung and double Compton scattering [2]. The problem is however complicated by the fact that the electron temperature enters the partial differential equation describing the evolution of photon intensity I_ν, or equivalently the photon occupation number $n(x) = c^2/(2h\nu^3)I_\nu$, itself depends on the photon spectrum [4, 5]

$$\frac{T_e}{T} = \frac{\int (n + n^2) x^4 dx}{4 \int n x^3 dx} \tag{A.1}$$

At high redshifts, when Compton scattering is able to establish Bose-Einstein spectrum, an analytic solution for the evolution of μ parameter accurate to $\sim 1\%$ can be found and is given by [2, 9]

$$\mu = 1.4 \int_{z_{\rm max}}^{z_\mu} {\rm d}z \left(\frac{dQ}{dz} - \frac{dQ}{dz}^{\rm cooling} \right) e^{-\mathcal{T}(z)} \tag{A.2}$$

where

$$\mathcal{T}(z) \approx 1.007 \left[\left(\frac{1+z}{1+z_{\rm dC}} \right)^5 + \left(\frac{1+z}{1+z_{\rm br}} \right)^{5/2} \right]^{1/2} + 1.007\epsilon \ln \left[\left(\frac{1+z}{1+z_\epsilon} \right)^{5/4} + \sqrt{1 + \left(\frac{1+z}{1+z_\epsilon} \right)^{5/2}} \right]$$
$$+ \left[\left(\frac{1+z}{1+z_{\rm dC}'} \right)^3 + \left(\frac{1+z}{1+z_{\rm br}'} \right)^{1/2} \right], \tag{A.3}$$

$$
\begin{aligned}
z_{\rm dC} &= \left[\frac{25\Omega_{\rm r}H(0)^2}{4C^2 a_{\rm C} a_{\rm dC}}\right]^{1/5}, & z_{\rm br} &= \left[\frac{25\Omega_{\rm r}H(0)^2}{4C^2 a_{\rm C} a_{\rm br}}\right]^{2/5} \\
z_\epsilon &= \left[\frac{a_{\rm br}}{a_{\rm dC}}\right]^{2/5}, & \epsilon &= \left[\frac{4C^2 {a_{\rm br}}^2 a_{\rm C}}{25 a_{\rm dC}\Omega_{\rm r}H(0)^2}\right]^{1/2}, \\
{z_{\rm dC}}' &= \left[\frac{3{\Omega_{\rm r}}^{1/2}H(0)}{2.958 C a_{\rm dC}}\right]^{1/3}, & {z_{\rm br}}' &= \left[\frac{{\Omega_{\rm r}}^{1/2}H(0)}{5.916 C a_{\rm br}}\right]^{2} \\
a_{\rm C} &= n_{\rm e0}\sigma_{\rm T} c \frac{k_{\rm B}T_{\rm CMB}}{m_{\rm e}c^2}, & a_{\rm dC} &= n_{\rm e0}\sigma_{\rm T} c \frac{4\alpha_{\rm fs}}{3\pi}\left(\frac{k_{\rm B}T_{\rm CMB}}{m_{\rm e}c^2}\right)^2 g_{\rm dC}(x_{\rm e}) I_{\rm dC} \\
a_{\rm br} &= n_{\rm e0}\sigma_{\rm T} c \frac{\alpha_{\rm fs} n_{\rm B0}}{(24\pi^3)^{1/2}}\left(\frac{k_{\rm B}T_{\rm CMB}}{m_{\rm e}c^2}\right)^{-7/2}\left(\frac{h}{m_{\rm e}c}\right)^3 g_{\rm br}(x_{\rm e}, T_{\rm e}),
\end{aligned}
\tag{A.4}
$$

$C = 0.7768$, $I_{\rm dC} \approx 25.976$, $g_{\rm dC} = 1.005$ and $g_{\rm br} = 2.99$, all quantities with subscript zero are evaluated at redshift $z = 0$, $\alpha_{\rm fs}$ is the fine structure constant and $\Omega_{\rm r}$ is the total radiation energy density parameter with relativistic neutrinos. The above equations assume that there is injection of only energy. If there is also significant injection of photons (other than bremsstrahlung and double Compton) then an additional term, $-2.404\frac{{\rm d}N}{{\rm d}z}$ must be added in the brackets in Eq. A.2, where N is the fractional change in the number density of photons. $z_{\rm max}$ should be taken to be sufficiently behind blackbody surface at $z_{\rm dC} \approx 1.96 \times 10^6$, $z_{\rm max} = 5 \times 10^6$ should be sufficient for most energy injection scenarios. z_μ is the boundary of transition from μ-type to i-type distortions and is discussed below. We have also accounted for the cooling of radiation because of energy transfer to baryons which cool faster than radiation with the expansion of the Universe and which has a simple expression before the start of the recombination [7, 22, 23, 49],

$$
\frac{dQ}{dz}^{\rm cooling} = \frac{3}{2}\frac{k_{\rm B}(n_{\rm H} + n_{\rm He} + n_{\rm e})}{a_{\rm R}T^3(1+z)}, \tag{A.5}
$$

where $n_{\rm H}$ and $n_{\rm He}$ are the number densities of hydrogen and helium nuclei.

For the i-type distortions we must solve the Kompaneets equation numerically. It turns out that the Kompaneets equation can be cast entirely in terms of dimensionless variables using y_γ as the time variable,

$$
y_\gamma(z, z_{\rm inj}) = -\int_{z_{\rm inj}}^{z} dz \frac{k_B\sigma_T}{m_e c}\frac{n_e T}{H(1+z)}, \tag{A.6}
$$

Solving Kompaneets equation with the initial spectrum corresponding to a y-type distortion, it was found[11] that the spectrum starts deviating from y-type distortion at 1% level at $y_\gamma = 0.01$ and is with 1% of a μ-type distortion at $y_\gamma = 2$. We thus define the boundaries of the i-type epoch by $y_\gamma(0, z_\mu) = 2$ and $y_\gamma(0, z_y) = 0.01$. At $z > z_\mu \approx 2 \times 10^5$ we have μ-type distortions and at $z < z_y \approx 1.5 \times 10^4$ we have y-type distortions.

The total distortion, excluding y-type, is now given by,

$$
\Delta I_\nu = \frac{2h\nu^3}{c^2}\left[\sum_i \frac{n_i}{Q_{\rm ref}}\left(\frac{dQ}{dz} - \frac{dQ}{dz}^{\rm cooling}\right)\frac{{\rm d}z}{{\rm d}y_\gamma}\delta y_{\gamma_i} + \mu n_\mu\right], \tag{A.7}
$$

where all terms are evaluated at redshift $z^i_{\rm inj}$ related to y_{γ_i} by $y_{\gamma_i} = y_\gamma(0, z^i_{\rm inj})$, the sum is over values of y_γ finely sampled between 0.01 and 2, $n_i(y_{\gamma_i})$ is the intermediate spectrum obtained by evolving y-type

distortion with energy $Q_{\rm ref}$ from $y_\gamma = 0$ to y_{γ_i} with Kompaneets equation, $\delta y_{\gamma_i} = (y_{\gamma_{i+1}} - y_{\gamma_{i-1}})/2$. The $i-$type spectra, n_i, sampled at intervals $\delta y_{\gamma_i} = 0.001$ for $y_\gamma < 1$ and $\delta y_{\gamma_i} = 0.01$ for $1 < y_\gamma < 10$ for $Q_{\rm ref} = 4 \times 10^{-5}$ are available at http://www.mpa-garching.mpg.de/~khatri/idistort.html along with a Mathematica code which implements the above recipe. The above formula simply calculates the energy injected in each small redshift interval and adds the appropriate distortion to the total. With the redshift/y_γ bins defined above the accuracy of the final spectrum is $\sim 1\%$. The most time consuming part of the above calculation is the calculation of $y_\gamma(0, z_{\rm inj})$ as a function of $z_{\rm inj}$, but it can be stored and reused if the normal cosmological parameters are not changing significantly.

Finally, y-type , μ-type and t-type occupation numbers are[5] [2, 6, 12]

$$\begin{aligned} n_y &= \frac{xe^x}{(e^x-1)^2}\left[x\left(\frac{e^x+1}{e^x-1}\right)-4\right] \\ n_\mu &= \frac{\mu e^x}{(e^x-1)^2}\left(\frac{x}{2.19}-1\right) \\ n_t &= \frac{xe^x}{(e^x-1)^2} \end{aligned} \tag{A.8}$$

References

[1] D. J. Fixsen, E. S. Cheng, J. M. Gales, J. C. Mather, R. A. Shafer, and E. L. Wright, *The Cosmic Microwave Background Spectrum from the Full COBE FIRAS Data Set*, *ApJ* **473** (1996) 576.

[2] R. A. Sunyaev and Y. B. Zeldovich, *The interaction of matter and radiation in the hot model of the Universe, II*, *ApSS* **7** (1970) 20–30.

[3] L. Danese and G. de Zotti, *Double Compton process and the spectrum of the microwave background*, *A&A* **107** (1982) 39–42.

[4] Y. B. Zeldovich and E. V. Levich, *Stationary state of electrons in a non-equilibrium radiation field.*, *Soviet Journal of Experimental and Theoretical Physics Letters* **11** (1970) 35–38.

[5] E. V. Levich and R. A. Sunyaev, *Heating of Gas near Quasars, Seyfert-Galaxy Nuclei, and Pulsars by Low-Frequency Radiation.*, *Soviet Astronomy* **15** (1971) 363.

[6] A. F. Illarionov and R. A. Sunyaev, *Comptonization, characteristic radiation spectra, and thermal balance of low-density plasma*, *Soviet Astronomy* **18** (1975) 413–419.

[7] J. Chluba and R. A. Sunyaev, *The evolution of CMB spectral distortions in the early Universe*, *MNRAS* **419** (2012) 1294–1314.

[8] P. Procopio and C. Burigana, *A numerical code for the solution of the Kompaneets equation in cosmological context*, *A&A* **507** (2009) 1243–1256.

[9] R. Khatri and R. A. Sunyaev, *Creation of the CMB spectrum: precise analytic solutions for the blackbody photosphere*, *JCAP* **6** (2012) 38.

[10] A. S. Kompaneets, *The establishment of thermal equilibrium between quanta and electrons*, *Zh. Eksp. Teor. Fiz.* **31** (1956) 876–875.

[11] R. Khatri and R. A. Sunyaev, *Beyond y and μ: the shape of the CMB spectral distortions in the intermediate epoch*, $1.5{\times}10^4 \lesssim z \lesssim 2{\times}10^5$, *JCAP* **9** (2012) 16.

[12] Y. B. Zeldovich and R. A. Sunyaev, *The Interaction of Matter and Radiation in a Hot-Model Universe*, *ApSS* **4** (1969) 301–316.

[5] These definitions are with respect to a reference blackbody which is defined by the photon number density, see [11, 40] for details.

[13] W. Hu, D. Scott, and J. Silk, *Reionization and cosmic microwave background distortions: A complete treatment of second-order Compton scattering*, *Phys.Rev.D* **49** (1994) 648–670.

[14] R. Cen and J. P. Ostriker, *Where Are the Baryons?*, *ApJ* **514** (1999) 1–6.

[15] R. Cen and J. P. Ostriker, *Where Are the Baryons? II. Feedback Effects*, *ApJ* **650** (2006) 560–572.

[16] B. B. Nath and J. Silk, *Heating of the intergalactic medium as a result of structure formation*, *MNRAS* **327** (2001) L5–L9.

[17] H. Trac, P. Bode, and J. P. Ostriker, *Templates for the Sunyaev-Zel'dovich Angular Power Spectrum*, *ApJ* **727** (2011) 94, [arXiv:1006.2828].

[18] N. Battaglia, J. R. Bond, C. Pfrommer, and J. L. Sievers, *On the Cluster Physics of Sunyaev-Zel'dovich and X-Ray Surveys. II. Deconstructing the Thermal SZ Power Spectrum*, *ApJ* **758** (2012) 75, [arXiv:1109.3711].

[19] L. D. Shaw, D. Nagai, S. Bhattacharya, and E. T. Lau, *Impact of Cluster Physics on the Sunyaev-Zel'dovich Power Spectrum*, *ApJ* **725** (2010) 1452–1465, [arXiv:1006.1945].

[20] K. Dolag and R. Sunyaev, *Relative velocity of dark matter and barions in clusters of galaxies and measurements of their peculiar velocities*, *ArXiv e-prints* (2013) [arXiv:1301.0024].

[21] The COrE Collaboration, *COrE (Cosmic Origins Explorer) A White Paper*, *ArXiv e-prints* (2011) [arXiv:1102.2181].

[22] Y. B. Zeldovich, V. G. Kurt, and R. A. Sunyaev, *Recombination of Hydrogen in the Hot Model of the Universe*, *Zh. Eksp. Teor. Fiz.* **55** (1968) 278.

[23] P. J. E. Peebles, *Recombination of the Primeval Plasma*, *ApJ* **153** (1968) 1.

[24] V. K. Dubrovich, *Hydrogen recombination lines of cosmological origin*, *Soviet Astronomy Letters* **1** (1975) 196.

[25] J. A. Rubiño-Martín, J. Chluba, and R. A. Sunyaev, *Lines in the cosmic microwave background spectrum from the epoch of cosmological hydrogen recombination*, *MNRAS* **371** (2006) 1939–1952.

[26] J. A. Rubiño-Martín, J. Chluba, and R. A. Sunyaev, *Lines in the cosmic microwave background spectrum from the epoch of cosmological helium recombination*, *A&A* **485** (2008) 377–393.

[27] K. Basu, C. Hernández-Monteagudo, and R. A. Sunyaev, *CMB observations and the production of chemical elements at the end of the dark ages*, *A&A* **416** (2004) 447–466.

[28] R. A. Sunyaev and R. Khatri, *Unavoidable CMB spectral features and blackbody photosphere of our Universe*, *ArXiv e-prints* (Feb., 2013) [arXiv:1302.6553].

[29] U. Seljak and M. Zaldarriaga, *A Line-of-Sight Integration Approach to Cosmic Microwave Background Anisotropies*, *ApJ* **469** (1996) 437.

[30] W. Hu and M. White, *The Damping Tail of Cosmic Microwave Background Anisotropies*, *ApJ* **479** (Apr., 1997) 568, [astro-ph/9609079].

[31] J. Silk, *Cosmic Black-Body Radiation and Galaxy Formation*, *ApJ* **151** (1968) 459.

[32] P. J. E. Peebles and J. T. Yu, *Primeval Adiabatic Perturbation in an Expanding Universe*, *ApJ* **162** (1970) 815.

[33] N. Kaiser, *Small-angle anisotropy of the microwave background radiation in the adiabatic theory*, *MNRAS* **202** (1983) 1169–1180.

[34] R. Hlozek et al., *The Atacama Cosmology Telescope: A Measurement of the Primordial Power Spectrum*, *ApJ* **749** (2012) 90.

[35] R. Keisler et al., *A Measurement of the Damping Tail of the Cosmic Microwave Background Power Spectrum with the South Pole Telescope*, *ApJ* **743** (2011) 28.

[36] Planck Collaboration, P. A. R. Ade, N. Aghanim, C. Armitage-Caplan, M. Arnaud, and et al., *Planck 2013 results. XVI. Cosmological parameters*, *ArXiv e-prints* (Mar., 2013) [arXiv:1303.5076].

[37] R. A. Daly, *Spectral distortions of the microwave background radiation resulting from the damping of pressure waves*, *ApJ* **371** (1991) 14–28.

[38] W. Hu, D. Scott, and J. Silk, *Power spectrum constraints from spectral distortions in the cosmic microwave background*, *ApJl* **430** (1994) L5–L8.

[39] J. Chluba, R. Khatri, and R. A. Sunyaev, *CMB at* 2×2 *order: the dissipation of primordial acoustic waves and the observable part of the associated energy release*, *MNRAS* **425** (2012) 1129–1169.

[40] R. Khatri, R. A. Sunyaev, and J. Chluba, *Mixing of blackbodies: entropy production and dissipation of sound waves in the early Universe*, *A&A* **543** (2012) A136.

[41] E. Pajer and M. Zaldarriaga, *A Hydrodynamical Approach to CMB mu-distortions*, *ArXiv e-prints* (2012) [arXiv:1206.4479].

[42] S. Weinberg, *Entropy Generation and the Survival of Protogalaxies in an Expanding Universe*, *ApJ* **168** (Sept., 1971) 175.

[43] G. Hinshaw et al., *Nine-Year Wilkinson Microwave Anisotropy Probe (WMAP) Observations: Cosmological Parameter Results*, *ArXiv e-prints* (Dec., 2012) [arXiv:1212.5226].

[44] C.-P. Ma and E. Bertschinger, *Cosmological Perturbation Theory in the Synchronous and Conformal Newtonian Gauges*, *ApJ* **455** (Dec., 1995) 7–+, [astro-ph/9506072].

[45] V. F. Mukhanov and G. V. Chibisov, *Quantum fluctuations and a nonsingular universe*, *Soviet Journal of Experimental and Theoretical Physics Letters* **33** (May, 1981) 532.

[46] A. Kosowsky and M. S. Turner, *CBR anisotropy and the running of the scalar spectral index*, *Phys.Rev.D* **52** (Aug., 1995) 1739, [astro-ph/9504071].

[47] W. Hu and N. Sugiyama, *Anisotropies in the cosmic microwave background: an analytic approach*, *ApJ* **444** (May, 1995) 489–506, [astro-ph/9407093].

[48] S. Dodelson, *Modern cosmology*. Modern cosmology / Scott Dodelson. Amsterdam (Netherlands): Academic Press. ISBN 0-12-219141-2, 2003.

[49] R. Khatri, R. A. Sunyaev, and J. Chluba, *Does Bose-Einstein condensation of CMB photons cancel* μ *distortions created by dissipation of sound waves in the early Universe?*, *A&A* **540** (2012) A124.

[50] S. Weinberg, *Cosmology*. Oxford University Press, Oxford, 2008.

[51] E. Pajer and M. Zaldarriaga, *New Window on Primordial Non-Gaussianity*, *Physical Review Letters* **109** (2012), no. 2 021302.

[52] J. Ganc and E. Komatsu, *Scale-dependent bias of galaxies and* μ*-type distortion of the cosmic microwave background spectrum from single-field inflation with a modified initial state*, *Phys.Rev.D* **86** (2012), no. 2 023518.

[53] A. van Engelen et al., *A Measurement of Gravitational Lensing of the Microwave Background Using South Pole Telescope Data*, *ApJ* **756** (Sept., 2012) 142, [arXiv:1202.0546].

[54] S. Das et al., *Detection of the Power Spectrum of Cosmic Microwave Background Lensing by the Atacama Cosmology Telescope*, *Physical Review Letters* **107** (July, 2011) 021301, [arXiv:1103.2124].

[55] L. Anderson et al., *The clustering of galaxies in the SDSS-III Baryon Oscillation Spectroscopic Survey: baryon acoustic oscillations in the Data Release 9 spectroscopic galaxy sample*, *MNRAS* **427** (Dec., 2012) 3435–3467, [arXiv:1203.6594].

[56] C. Blake et al., *The WiggleZ Dark Energy Survey: joint measurements of the expansion and growth history at z ¡ 1*, *MNRAS* **425** (Sept., 2012) 405–414, [arXiv:1204.3674].

[57] F. Beutler et al., *The 6dF Galaxy Survey: baryon acoustic oscillations and the local Hubble constant*, *MNRAS* **416** (Oct., 2011) 3017–3032, [arXiv:1106.3366].

[58] A. Sandage et al., *The Hubble Constant: A Summary of the Hubble Space Telescope Program for the Luminosity Calibration of Type Ia Supernovae by Means of Cepheids*, *ApJ* **653** (Dec., 2006) 843–860, [astro-ph/0603647].

[59] W. L. Freedman et al., *Carnegie Hubble Program: A Mid-infrared Calibration of the Hubble Constant*, *ApJ* **758** (Oct., 2012) 24, [arXiv:1208.3281].

[60] A. G. Riess et al., *A 3% Solution: Determination of the Hubble Constant with the Hubble Space Telescope and Wide Field Camera 3*, *ApJ* **730** (Apr., 2011) 119, [arXiv:1103.2976].

[61] A. Conley et al., *Supernova Constraints and Systematic Uncertainties from the First Three Years of the Supernova Legacy Survey*, *ApJS* **192** (Jan., 2011) 1, [arXiv:1104.1443].

[62] M. Sullivan et al., *SNLS3: Constraints on Dark Energy Combining the Supernova Legacy Survey Three-year Data with Other Probes*, *ApJ* **737** (Aug., 2011) 102, [arXiv:1104.1444].

[63] G. Mangano, G. Miele, S. Pastor, T. Pinto, O. Pisanti, and P. D. Serpico, *Relic neutrino decoupling including flavour oscillations*, *Nuclear Physics B* **729** (2005) 221–234.

[64] A. Kogut, D. J. Fixsen, D. T. Chuss, J. Dotson, E. Dwek, M. Halpern, G. F. Hinshaw, S. M. Meyer, S. H. Moseley, M. D. Seiffert, D. N. Spergel, and E. J. Wollack, *The Primordial Inflation Explorer (PIXIE): a nulling polarimeter for cosmic microwave background observations*, *JCAP* **7** (2011) 25.

[65] M. Tegmark, A. N. Taylor, and A. F. Heavens, *Karhunen-Loeve Eigenvalue Problems in Cosmology: How Should We Tackle Large Data Sets?*, *ApJ* **480** (May, 1997) 22, [astro-ph/9603021].

[66] T. Matsubara, *Correlation Function in Deep Redshift Space as a Cosmological Probe*, *ApJ* **615** (Nov., 2004) 573–585, [astro-ph/0408349].

[67] A. Albrecht et al., *Findings of the Joint Dark Energy Mission Figure of Merit Science Working Group*, *ArXiv e-prints* (Jan., 2009) [arXiv:0901.0721].

[68] A. Lewis and S. Bridle, *Cosmological parameters from CMB and other data: A Monte Carlo approach*, *Phys.Rev.D* **66** (Nov., 2002) 103511, [astro-ph/0205436].

[69] D. Larson et al., *Seven-year Wilkinson Microwave Anisotropy Probe (WMAP) Observations: Power Spectra and WMAP-derived Parameters*, *ApJS* **192** (2011) 16.

[70] C. L. Reichardt et al., *A Measurement of Secondary Cosmic Microwave Background Anisotropies with Two Years of South Pole Telescope Observations*, *ApJ* **755** (Aug., 2012) 70, [arXiv:1111.0932].

[71] S. Das et al., *The Atacama Cosmology Telescope: Temperature and Gravitational Lensing Power Spectrum Measurements from Three Seasons of Data*, *ArXiv e-prints* (Jan., 2013) [arXiv:1301.1037].